Mechanism of Action for Promensil in Regard to T47D Cell Proliferation

A Major Qualifying Project Report
Worcester Polytechnic Institute
Department of Biology and Biotechnology

Advisors: Mike Buckholt, PhD
Jill Rulfs, PhD

Author: Sarah Huber

Table of Contents

Abstract

Promensil is an over-the-counter phytoestrogen supplement marketed to menopausal women as an alternative to hormone replacement therapy. Prior studies looking into the relationship between Promensil and breast cancer have yielded inconsistent results, so the goal of this study was to investigate the relationship between Promensil and cell proliferation in an estrogen receptor-positive breast epithelial cell line. It was found that introducing Promensil to T47D cells correlated to decreased cell counts, and markers for the cell cycle, DNA replication, and apoptosis were followed to investigate the mechanism behind this decrease. Future studies should investigate the receptor status of the triple negative control line used and should explore the protein expression in this line as well.

Acknowledgements

I would like to thank my advisors, Professors Jill Rulfs and Mike Buckholt for guiding me through this project, and a special thank you to Jill Rulfs for splitting my cells on days when I could not come into the lab and for maintaining back up stocks of cell lines throughout the duration of this project.

Background

Introduction

Phytoestrogens are plant derived molecules that structurally mimic endogenous estrogens. Because of their structural similarity to estrogens, phytoestrogen over the counter supplements, such as Promensil, have largely been marketed as safer alternatives to hormone replacement therapy for women with menopause, since HRT has been shown to have a strong correlation with the risk of developing breast cancer. However, there is an abundance of conflicting data in regard to the relationship between phytoestrogens and breast cancer incidence – specifically, in regard to whether or not phytoestrogens increase or decrease cell proliferation in estrogen receptor-positive breast cancer cells. Previous undergraduate studies at WPI have found a relationship between phytoestrogens and antiproliferative effects in estrogen receptor-positive breast cancer cell lines, but the mechanism of action behind this decreased cell growth is still largely unknown. As such, the overall goal for this study was to determine the mechanism through which Promensil can affect proliferation in T47D ER-positive cells by examining its potential to interact with and affect estrogen receptors and key molecules in the cell cycle, DNA replication, and apoptosis pathways.

Breast Cancer

Breast cancer is the second most common cancer for women in the United States. In fact, according to the CDC, in 2017, female breast cancer had the highest rate of new cases in the United States and was second only to lung cancer in terms of cancer death rates in the United States (Centers for Disease Control [CDC], n.d.).

Breast cancers can be classified based on their responsiveness to hormones. Specifically, breast cancer can either be estrogen receptor (ER) positive or negative. In ER-positive breast cancers, the tumorigenic cells contain ERs and proliferate through the binding of estrogen to these receptors. In fact, almost 80% of breast cancers are ER-positive (National Cancer Institute, 2017). ER-positive breast cancer was the focus of this study, and the interactions between ER-positive breast cancer cells and phytoestrogens was investigated. An ER-negative cell line was also maintained and served as a negative control line for this study.

Estrogen

Estrogen is an endogenous steroidal hormone that is mainly responsible for regulating the female reproductive system. As such, estrogen is responsible for triggering the development of female secondary sex characteristics during puberty, such as larger breasts and pubic hair (“Estrogen,” 2018). Moreover, estrogen levels are regularly controlled during a female’s peak reproductive years via a negative feedback loop consisting of estrogen, follicle stimulating hormone (FSH), luteinizing hormone (LH), and progesterone. Estrogen is released from the ovaries in response to the presence of FSH. Once estrogen levels reach a specific threshold, LH then triggers the release of an ovum from the ovaries, and progesterone levels rise to prepare the uterus for pregnancy. If the ovum does not become fertilized, the uterus begins to shed as menstruation

begins, and hormone levels essentially reset to begin the cycle again (Harvard Health Publishing, n.d.). Additionally, estrogen plays a role in the maintenance of many other physiological systems, such as the neuroendocrine, vascular, skeletal, and immune systems (Hamilton, et. al., 2017). The main form of ovarian estrogen in females is 17β-estradiol (E2), which is the estrogen that was introduced in the present study as a positive control ("Estradiol," 2005) (Figure 1).

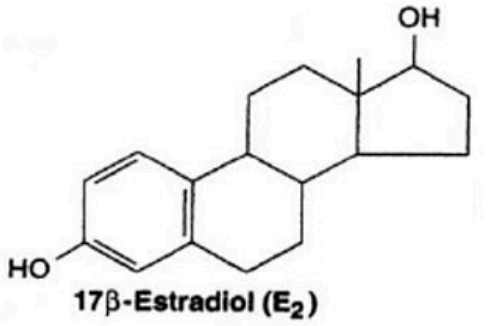

Figure 1: "Male (left) and female (right) hormones (Ganong, 2005, pg.429, pg.440).jpg" by Amanda CXV is licensed under CC BY-SA 4.0.

Since E2 is the estrogen most responsible for the development of breast tissue during female puberty and is most active during sexual maturity, it is an appropriate molecule for breast cancer research, specifically for ER-positive cancers. Because E2 plays such a large role in the development of breasts, a surge in this hormone is key in tumor formation in the breast tissue in ER-positive breast cancers, making high levels of this hormone potentially dangerous. In fact, E2 has shown carcinogenic effects in MCF-10F1 nontumorigenic mammary cells and has been shown to induce adenocarcinomas in rats when administered in high doses (ATCC, n.d., Russo, et.al., 2006, Russo & Russo, 1996).

Estrogen has two naturally occurring receptors coded for by different genes present on separate chromosomes: ER-α and ER-β (Couse & Korach, 1999). Both ER-α and ER-β are steroidal nuclear receptors, and when bound to estrogen act as transcriptional activators to regulate a number of physiological pathways via the cell cycle. In other words, Both ER-α and ER-β function as activator molecules that when bound to E2 interact with regulatory sites on DNA called estrogen response elements (EREs). This interaction is achieved in one of two ways: the ER-E2 complex either binds directly to an ERE, directly mediating an interaction with RNA polymerase and triggering the transcription of the target gene, or the complex interacts with a different transcription factor via a "tethering" interaction, therefore not binding directly to the DNA (Klinge, 2001).

The specific roles of ER-α and ER-β have been extensively investigated using knockout mice, in which it was found that these two receptors have opposite biological functions (Lee, et. al., 2012). Specific to breast cancer, generally ER-α has been shown to increase cancer cell proliferation, whereas ER-β plays an anti-proliferative role (Paterni, et. al., 2014). Moreover, the binding of estrogen to ER-α has been shown to recruit proliferating cell nuclear antigen (PCNA), a molecule that helps the expression of genes that contribute to increased cellular proliferation (Shultz-Norton, et. al., 2007). PCNA functions as an important molecule in facilitating DNA

replication and thus cell proliferation by binding to and recruiting additional replication factors and acting as a sliding polymerase clamp (Boehm, et. al., 2016).

In addition to their contrasting roles, the two estrogen receptors also have different localizations within the body. Specifically, ER-α and β are found in different tissues with a vast dispersion throughout the body. Whereas ER-α is located in the cells of the uterus, mammary gland, testes, pituitary gland, liver, kidney, heart, and skeletal muscle, ER-β is localized to the ovaries and prostate. Additionally, in tissues that contain both ERs, there is also a discrete localization of the receptors, which serves to reinforce their different biological functions (Couse & Korach, 1999). For example, immunohistochemical localization studies have demonstrated a localization of ER-α to the thecal cells in rat ovaries, whereas ER-β has mainly been shown to be localized to the granulosa cells (Sar & Welsch, 1999).

Menopause

Menopause is defined as the time twelve months following a woman's final menstrual cycle (Mayo Clinic, 2020). During menopause, the ovaries stop producing progesterone and estrogen, terminating both menstruation and the ability to become pregnant. In response to the lack of estrogen and progesterone, symptoms of menopause may include hot flashes, night sweats, vaginal dryness, incontinence, trouble sleeping, decreased sex drive, and mood changes (National Institute of Health [NIH], n.d.).

Because menopause is brought about by a decline in progesterone and estrogen, hormone replacement therapy (HRT) has been a common menopausal treatment since the 1960s, although its popularity has since declined with the discovery of the relationship between HRT and the incidence of breast cancer (Cagnacci & Venier, 2019). HRT for menopause includes oral, transdermal, and internal treatment with estrogen, progesterone, or a combination of the two hormones (Banks, et. al., 2003). Although it has proven efficient as a treatment for menopause, the use of HRT has been shown to have a very strong positive correlation with the risk of breast cancer incidence and fatality, as shown in the highly cited Oxford University "Million Women Study" (Banks, et. al., 2003).

Phytoestrogens

Phytoestrogens are molecular plant-derivatives present in plants like legumes and red clover, with structures that mimic naturally occurring human endogenous estrogens. Two common classes of phytoestrogens are lignans and isoflavones (Křížová, et. al., 2019). Phytoestrogens are largely marketed as over the counter supplements for use as alternatives to HRT to help alleviate symptoms in menopausal women through products such as Promensil. Phytoestrogens are often labeled as "safe" alternatives to HRT due to the correlation observed between a low risk of breast cancer in Asian countries and high consumption of soy in Asian diets, which is naturally rich in phytoestrogens (Sakamonto, et. al. 2015, Xu, et. al., 1998). Moreover, another interesting correlational study found that there exists a relationship between a decreased risk for both pre and postmenopausal breast cancer and a urinary excretion of isoflavones and lignans, suggesting again that dietary consumption (and therefor urinary excretion) of phytoestrogens is linked to low breast cancer risk (Ingram, et al., 1997). However, it is important to note that these two

claims are based purely on correlation, and there also exist many experimental studies related to the "safeness" of phytoestrogen supplements as a HRT replacement which have had more conflicting results.

Because phytoestrogens mimic natural estrogens in molecular structure, it has been proposed that they also have the potential to alter cell proliferation in ER-positive breast tissue by binding to either ER-α or ER-β and acting as either estrogen receptor agonists or antagonists. In fact, many studies have looked into the role that phytoestrogens play in estrogenic pathways and the implications these interactions have for breast cancer, although the results have been largely varied. For instance, it was found through a placebo-controlled trial that consumption of red clover isoflavones did not result in any difference in breast cancer risk relative to the control on a number of breast cancer risk markers, such as breast density, suggesting they may have no effect on breast cancer incidence (Atkinson, et. al. 2004). Additionally, another study found that when MCF-7 ER-positive breast cancer cells were treated with four different phytoestrogens, each compound had a slightly different effect on tumorigenesis, cell proliferation, and apoptosis, lending to a lot of ambiguity in regard to phytoestrogens' mechanism as a whole (Sakamonto, et. al., 2015). However, a different study found that enterolactone (a metabolite from lignans) was able to decrease tumorigenesis in MDA-MB-231 triple negative breast cancer cells by interfering with the cell cycle to arrest cells at the S phase and altering the expression of proliferation-dependent genes (Xiong, et. al., 2015). On the other hand, in yet another study, soy isoflavone extracts were actually found to increase the expression of Ki-67, a nuclear antigen responsible for proliferation, in healthy premenopausal women at risk for breast cancer (Khan, et. al., 2012). As suggested by the abundance of conflicting results in the literature, much is still unknown about the consequences of taking phytoestrogen supplements in regard to the risk of developing breast cancer, as some studies have suggested phytoestrogens can increase risk and incidence in both ER-positive and negative breast cells, whereas others have suggested they may decrease risk, and some say they have no effect at all. Moreover, it is possible that both carcinogenic and anticarcinogenic effects are achieved through the introduction of different phytoestrogens to breast cells, or that these effects are different in cells that have estrogen receptors and those that do not.

Promensil

Promensil is a popular phytoestrogen supplement that contains phytoestrogen extracts from red clover. Specifically, Promensil contains extracts from four isoflavones: daidzein, genistein, biochanin A, and formononetin ("About Promensil," n.d.) (Figure 2).

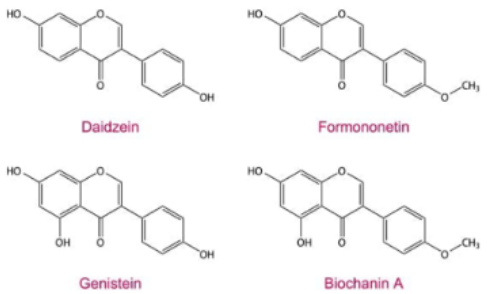

Figure 2: Isoflavones in Promensil (via https://Promensil.co.uk/about/)

According to the Promensil product site, supposedly Promensil has no affinity for ER-α and works to alleviate menopausal symptoms by binding to ER-β and mimicking the effects of endogenous estrogen ("About Promensil," n.d.). Because the binding of ER-β to estrogen typically has antiproliferative effects in ER-positive breast cancers, assuming this claim to be true, it would be suspected that Promensil may then decrease the risk of breast cancer incidence by acting as an agonist to ER-β.

Several previous WPI undergraduate studies (known as Major Qualifying Projects, or "MQPs") have looked into the interactions between both ER-α and β and Promensil extracts and have all resulted in one common finding: the overall result of introducing Promensil has been an observed decrease in cell proliferation in both ER-positive and negative cell lines. However, none of these studies have been able to support the claim from the Promensil product site that Promensil is an estrogen agonist with a specific affinity for ER-β. In fact, in 2018, one MQP focused on the role of ER-β specifically and its role in contributing to the antiproliferation observed with the introduction of Promensil to an ER-positive breast cancer cell line. By manipulating an ER-β tunable cell line and shutting off the ER-β receptor with tetracycline, it was determined that this had no effect on the observed proliferation relative to the control when Promensil was present (Wambach, 2018). A follow up study in 2019 then aimed to investigate the relationship between ER-α and Promensil, hypothesizing that since the previous study suggested Promensil does not act through ER-β, it might act as an ER-α antagonist to decrease cell proliferation. However, this study also did not find any changes to proliferation when ER-α was active versus when it was inhibited with methyl-piperidino-pyrazole (MPP) and Promensil was introduced (Aquino, et. al., 2019). Overall, both of these studies suggested that Promensil may not act through either receptor and may therefor decrease proliferation via some other mechanism.

Most recently, a 2020 MQP found these results unconvincing, since previous research with luciferase assays had indicated prior that Promensil does in fact interact with estrogen receptors in some manner. As such, it was then suggested that it seemed unlikely that shutting off both ER-α and ER-β would not affect proliferation in the presence of Promensil. To test this assumption, in this study both ER-α and ER-β were blocked simultaneously, but again no change in proliferation was observed (Jankowski, et. al., 2020). As such, this present study was done as a means to follow up on these previous three projects, with the goal being to investigate this observed antiproliferation in relation to both ER-dependent pathways as well as ER-independent mechanisms, such as the cell cycle, DNA replication, and apoptosis.

It is important to note that with the one commonality stemming from these past WPI projects being that Promensil correlated to a decrease in cell proliferation, the possibility cannot be overlooked that this decrease in cell proliferation may not be due to the phytoestrogens within the supplement at all. Phytoestrogen-derived menopausal supplements contain many other compounds other than the phytoestrogen molecules themselves. For Promensil specifically, the first ingredient on the product label is listed as unclassified "bulking agents." Thus, it is possible that the consistently observed decrease in cell proliferation could be caused by some non-phytoestrogen molecule interacting with the estrogenic pathway via binding to ERs, which

would explain the results to the previous luciferase assays, or the antiproliferation could be caused by the phytoestrogens acting through other pathways and not binding to ERs at all.

The Cell Cycle

In general, decreased cellular proliferation is the result of inhibiting cellular growth by either arresting the cell cycle or by increasing apoptosis. As such, since it has been the consistent finding in previous undergraduate WPI studies that introducing Promensil to ER-positive breast cancer cell lines results in a decreased cellular proliferation, both arresting the cell cycle and increasing apoptosis provide possible mechanisms for this observation.

Cellular function is largely dependent on the coordination of the cell cycle in response to internal and external stimuli. Regulatory molecules are responsible for the coordination of the cell cycle through its growth and replication phases. Namely, two molecules that play a large role in the cell cycle are cyclins and cyclin dependent kinases (CDKs). Cyclin-CDK activity influences the cell cycle through interactions at restriction points (R points). Specifically, the binding of cyclins to CDKs at R points triggers conformational changes that progress the cell cycle via phosphorylation of molecules responsible for cell proliferation. For example, at the G1 checkpoint, cyclin-CDK activity phosphorylates the inhibitory tumor suppressor protein retinoblastoma (Rb), triggering its release from DNA and allowing proliferation to proceed (Ding, et. al., 2020).

CDK inhibitors (CKIs) also play a role during the cell cycle in response to physiological stressors. One important CKI is the p21 protein. p21 is a nonspecific CKI that can interfere with many cyclin-CDK complexes at every R point in the cell cycle (Giacinti & Giordano, 2006). For example, p21 may be present at the G1 checkpoint if DNA is damaged. p21 will then interfere with the specific cyclin-CDK interactions at this R point by binding to the cyclin D-CDK4/6 complex, ultimately halting the cell cycle until the DNA damage can be repaired (Weinberg, 2014). p21 can also inhibit PCNA and halt DNA synthesis even if it is already occurring so that DNA can be repaired (Weinberg, 2014). The presence of p21 in a cell line can therefor indicate if decreased proliferation is due to the arresting of the cell cycle at one of these R points.

Apoptosis

Apoptosis, or programmed cell death, has important implications for healthy organismal development and routine cellular maintenance, whereby cells that cannot repair necessary damage are instructed to die. Several key molecules are involved in the apoptosis pathway in mammalian cells. In particular, p53 is a well-known and studied tumor suppressor protein that has a role in the cell cycle and can trigger apoptosis if necessary. Like p21, p53 triggers the halt of the cell cycle, but unlike p21 can also lead to apoptosis if necessary (Weinberg, 2014).

Bcl-2 is another molecule that has a large role in apoptosis, but with an opposing role to p53. In brief, Bcl-2 serves to block apoptosis in healthy cells. Bcl-2 is normally embedded in the outer mitochondrial membrane, and harbors cytochrome c in the intermembrane space. Cytochrome c normally plays a role in oxidative phosphorylation during cellular respiration, but when apoptosis is triggered, cytochrome c is released into the cytosol and participates in a cellular

signaling pathway that ultimately leads to apoptosis of the cell. In order for cytochrome c to be released, Bcl-2 has to be inactivated, which is ultimately caused by p53 transcriptionally activating relatives of Bcl-2 that can open the Bcl-2 channels. Once released into the cytoplasm, cytochrome c triggers a cascade of procaspases, activating them into their active caspase form. Caspases are a class of proteases that are heavily involved in the apoptosis pathway. Specific caspases called "executioner caspases" are responsible for the degradation of the nuclear membrane, fragmentation of nuclear DNA, cleavage of the cytoskeleton proteins, and further damage of the mitochondria, ultimately killing the cell (Weinberg, 2014). Caspase 3 is one such of these caspases, and its presence can indicate a dying cell.

Cell Lines

The T47D cell line was the main focus of this study. This line was derived from human breast epithelial cells extracted from a ductal carcinoma of a 54-year-old woman (ATCC, n.d.). T47D cells are estrogen-responsive and can be used to study ER-positive breast cancer *in vitro.* This cell line was used to simulate the effects of Promensil on ER-positive breast cells *in vivo*. MDA-MB-231 cells were also obtained from the ATCC and maintained and used as a negative control line. These cells are triple-negative breast cancer cells (breast cancer cells that lack both estrogen and progesterone receptors) and were initially obtained from a pleural effusion of a 51-year old woman with metastatic mammary adenocarcinoma (European Collection of Authenticated Cell Cultures [ECACC], 2017).

Hypothesis

Since the preceding WPI studies have displayed fairly consistent findings regarding Promensil's antiproliferative effects in ER-positive breast cancer cells, but inconclusive findings related to the mechanism of action involving ER-α and ER-β, it was hypothesized that Promensil is not acting through these receptors alone to cause antiproliferation. Instead, it was suspected that Promensil may decrease proliferation in estrogen-responsive breast cancer cells by acting in part through ERs and in part through non-estrogenic pathways. Specifically, it was hypothesized that Promensil may be involved in halting the cell cycle and reducing DNA replication via the upregulation of p21 and downregulation of PCNA, and may also be involved in triggering apoptosis via the upregulation of caspase 3. This hypothesis was derived in part by data that suggests that phytoestrogens can also decrease tumorigenesis in triple negative breast cancers as well, which lack both ER-α and ER-β. (Xiong, et. al., 2015).

Methods

Extraction of Promensil

To extract the phytoestrogens from Promensil, the same protocol was followed as the previous WPI undergraduate studies done by Wambach and Aquino et. al. in 2018 and 2019, respectively. This was done to ensure that the protocols used in these previous studies were followed as closely as possible, since this study was done as a continuation of this research. Three double strength Promensil tablets were crushed using a mortar and pestle. The powder was then combined with 100 mL of 80% methanol (MeOH) in a round bottom flask and allowed to reflux in an 18^{o}C water bath for one hour. The solution was then vacuum filtered and transferred into two 50 mL conical tubes for storage at -20^{o}C until use. After thawing and prior to use in experimental treatments, the solution was sterilized using a 0.22 μM filter unit.

Cell Maintenance

T47D breast epithelial cells were obtained from the ATTC and maintained according to their recommendations. The cells were grown in DMEM with L-glutamine plus 10% Fetal Bovine Serum (FBS), 1% penicillin/streptomycin (P/S), and 0.08% bovine insulin (0.2 units/mL of media, using insulin from bovine pancreas with a concentration of 10 mg/mL with a conversion of approximately 25 units/mg) (ATCC, n.d., Sigma Aldrich, n.d.). The cultures were kept in T75 culture flasks containing a total of 10 mL of media and kept in an incubator at 37^{o}C with 5% carbon dioxide. The cells were split as needed when they reached about 70-90% confluence (Figure 3), approximately twice a week. The media was also replaced every 2-3 days to keep cells in log phase growth conditions.

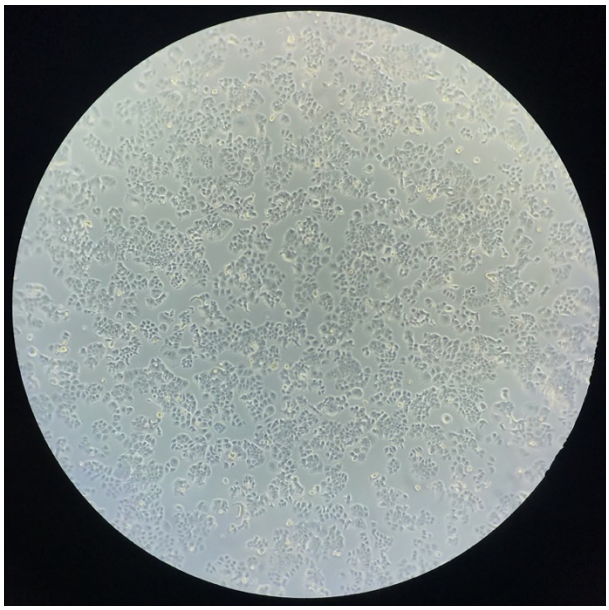

Figure 3: T47D cells under normal growth conditions in a T75 flask. The media used for normal growth conditions was DMEM + 10% FBS, 1% P/S, 0.08% insulin. The cells pictured are at approximately 70% confluence. This is the approximate density at which cells were normally split.

MDA-MB-231 triple negative breast epithelial cells were also obtained from the ATCC. These cells were maintained in DMEM plus 10% FBS and 1% P/S. These cells were also kept in T75 flasks and routinely split as needed (Figure 4).

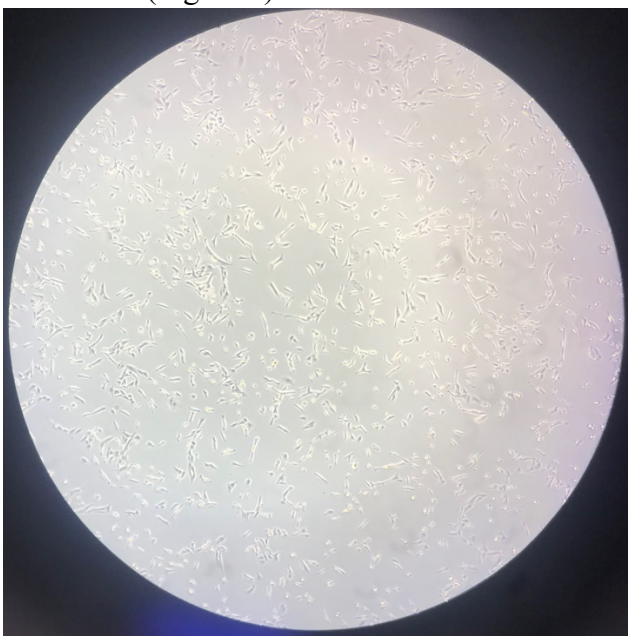

Figure 4: MDA-MB-231 cells under normal growth conditions in a T75 flask. The media used for normal growth conditions was DMEM + 10% FBS, 1% P/S. The cells pictured are at approximately 50% confluence.

Cell Plating and Cell Cycle Synchronization

Prior to all experiments, cells were trypsinized and transferred from T75 flasks to either 24-well plates at a plating density of approximately $0.05x10^6$ live cells or 12 well-plates at a plating density of approximately $0.1x10^6$ live cells, dependent on the experiment that was to be done. The media in these wells was held at a total volume of 1 mL for the 24-well plates, and 1.5 mL for the 12-well plates.

Prior to introducing any experimental treatments, the cells were first synchronized to the same stage in the cell cycle. This was achieved by allowing the cells to adhere to the well plates for 24 hours in DMEM with L-glutamine plus 10% FBS, 1% P/S, and 0.08% insulin (or media lacking insulin for the MDA-MB-23 cells). After 24 hours, this media was aspirated off and replaced with media lacking serum (DMEM + 1% P/S, 0.08% insulin for T47D cells). For the negative control cell line (MDA-MB-231), the cell-synchronization media was DMEM + 1% P/S only, and the introduction of this cell-synchronization media did not replace the standard media until 72 hours after adjustment to the well plate, rather than 24 hours. Waiting 72 hours to add the cell-synchronization media rather than 24 for this cell line was chosen because the MDA-MB-231 cells seemed to take longer to fully adhere to the bottom of the wells after the cells were initially introduced when compared to the time it took the T47D cells to adhere.

Experimental Conditions

After 24 hours of cell cycle synchronization, the serum-free media was aspirated off and replaced with media lacking phenol red and with charcoal stripped FBS (phenol red-free DMEM + 10% charcoal stripped FBS, 1% P/S, 0.08% insulin for T47D cells, and phenol red-free DMEM + 10% charcoal stripped FBS, 1% P/S for the MDA-MB-231 cells). The use of phenol red-free DMEM for the experimental media was because phenol red has shown to have the ability to bind to and stimulate ERs in several breast cancer cell lines, including T47D (Welshons, et. al., 1988). Additionally, using charcoal stripped FBS rather than the standard FBS was to ensure that any naturally occurring steroid molecules in the serum were removed, as these could also interact with ERs.

After the experimental media was introduced, the cells were again left to adjust to this new media for another 24 hours. After these 24 hours of adjustment, treatments were then added in varied amounts to the wells, depending on the well plate used (Tables 1 and 2), and the cells were allowed to incubate with their treatments for 72 hours. The experimental treatments were a varied concentration of the Promensil extract dissolved in 80% MeOH. The positive control treatment was an extract of 100nM 17β-estradiol (E2), and the negative control treatments were 80% MeOH and a media only control.

Cell Counts

After 72 hours of adjustment to the experimental conditions, the cells were trypsinized and harvested from the wells of 24-well plates to perform cell counts. All cell counts were performed using the Cellometer Automatic T4 Cell Counter. A layout of the experimental treatments introduced to the cells prior to cell counts can be seen in Table 1.

Table 1: Set up for experimental treatments and controls introduced to T47D and MDA-MB-231 cells after plating and prior to cell counts. The boxes represent wells in a 24-well plate. All cells were first synchronized to the same stage in the cell cycle by the addition of serum-free media (DMEM + 1% P/S, 0.08% insulin for the T47D cells and DMEM + 1% P/S for the MDA-MB-231 cells). Following, all cells were maintained in experimental media (phenol red-free DMEM + 10% charcoal stripped FBS, 1% P/S, 0.08% insulin for the T47D cells and phenol red-free DMEM + 10% charcoal stripped FBS, 1% P/S for the MDA-MB-231 cells) prior to and after the addition of the E2 control or Promensil treatments. The introduction of 80% MeOH to the Promensil treatments was because the Promensil extract was maintained in 80% MeOH. Holding the concentration of MeOH constant across each well served as a control for MeOH, so it could be ruled out that any changes between cells treated with different volumes of Promensil extract was due to the Promensil itself and not the MeOH solute.

Media only control	100nM Estradiol Positive Control + **20** µL 80% MeOH	**5** µL Promensil + **15** µL 80% MeOH	**10** µL Promensil + **10** µL 80% MeOH	**15** µL Promensil + **5** µL 80% MeOH	**20** µL Promensil
Media only control	100nM Estradiol Positive Control + **20** µL 80% MeOH	**5** µL Promensil + **15** µL 80% MeOH	**10** µL Promensil + **10** µL 80% MeOH	**15** µL Promensil + **5** µL 80% MeOH	**20** µL Promensil
Media only control	100nM Estradiol Positive Control + **20** µL 80% MeOH	**5** µL Promensil + **15** µL 80% MeOH	**10** µL Promensil + **10** µL 80% MeOH	**15** µL Promensil + **5** µL 80% MeOH	**20** µL Promensil

Immunodetection

Immunodetection was done on T47D cells after treatments with the E2 and Promensil extract. After 72 hours of adjustment to the experimental conditions, the media was aspirated off of the T47D cells and they were scraped off of a 12-well plate. A layout of the experimental treatments introduced to the cells prior to harvesting for immunodetection can be seen in Table 2. The amount of Promensil and MeOH introduced to the cells was increased prior to immunoblotting relative to the amount introduced prior to the cell counts, proportional to the media increase in the 12-well plates over the 24-well plates.

Table 2: Set up for experimental treatments and controls introduced to T47D cells after plating and prior to immunodetection. The boxes represent wells in a 12-well plate. All cells were first synchronized to the same stage in the cell cycle by the addition of serum free media (DMEM + 1% P/S, 0.08% insulin). Following, all cells were maintained in experimental media (phenol red-free DMEM + 10% charcoal stripped FBS, 1% P/S, 0.08% insulin) prior to and after the addition of the E2 control or Promensil treatments. The introduction of 80% MeOH to the Promensil treatments was because the Promensil extract was maintained in 80% MeOH. Holding the concentration of MeOH constant across each well served as a control for MeOH, so it could be ruled out that any changes between cells treated with different volumes of Promensil extract was due to the Promensil itself and not the MeOH solute.

Media only control	100nM Estradiol Positive Control + **30** µL 80% MeOH	**7.5** µL Promensil + **22.5** µL 80% MeOH
15 µL Promensil + **15** µL 80% MeOH	**22.5** µL Promensil + **7.5** µL 80% MeOH	**30** µL Promensil

After scraping, the cells were resuspended in 250 µL of PBS and frozen to lyse the cells. Protein assays were then performed to determine the total protein concentration in each sample after treatments to determine adequate membrane loading volumes for slot blots. To perform the slot blots, triplicate aliquots of 20µg of total protein from each treatment sample was transferred onto an immobilon membrane soaked with 100% MeOH and rinsed with TBS (10mM Tris, 0.9% NaCl). After transfer, the membrane was submerged in 100% MeOH for 10 seconds and then placed in a 37^{o}C incubator for 15 minutes to completely dry the membrane. The membrane was then cut in three pieces prior to incubation with one of the three primary antibodies to be used, so that each membrane had a sample of cells from each treatment group. The primary antibodies used for immunodetection were obtained from Santa Cruz Biotechnology and were used for the detection of PCNA (sc-25280), p21 (sc-6246), and caspase 3 (sc-271028). The antibodies were diluted 1:200 in a blocking solution of PBS + 1% BSA, 0.05% Tween. The membranes were incubated with primary antibody for one hour at room temperature with agitation. Following, membranes were rinsed twice with PBS for 10 seconds each. The membranes were then incubated for 30 minutes with secondary antibody at room temperature with agitation. The secondary antibody used was a rabbit-anti mouse antibody diluted 1:5,000 in blocking solution. The membranes were then again washed twice with PBS and then developed with SIGMA*FAST* BCIP/NBT developer (Sigma Aldrich, n.d.). After developing, photos were taken of each membrane, converted to TIFF files using ImageJ software, and densitometry analysis was done using the Biorad Image Lab software to quantify the expression levels of each target protein (Biorad, n.d.).

Results and Discussion

T47D Cell Morphologies and Density After Treatments

Prior to harvesting the T47D cells for counts, after 72 hours of adjustment to the treatments the cells in each treatment group were observed under an inverted microscope to determine if any distinct differences in cell morphology or density between the treatment groups were observable. Differences in cell morphology between the controls (media only control and 100nM E2 positive control) and the experimental groups (Promensil treatment groups of varied concentrations) can be seen in Figure 5. There were no large observable differences between the groups, except that for the cells introduced to the Promensil, small green particles could be observed in the media after 72 hours of incubation. It was suspected that these particles were ingredients in the Promensil product that are insoluble in MeOH. This was suspected because the Promensil extract solution was a dark green color, and there are several unknown ingredients in Promensil, as indicated by the listing of "bulking agents" on the product label, some of which were expected to be insoluble in MeOH.

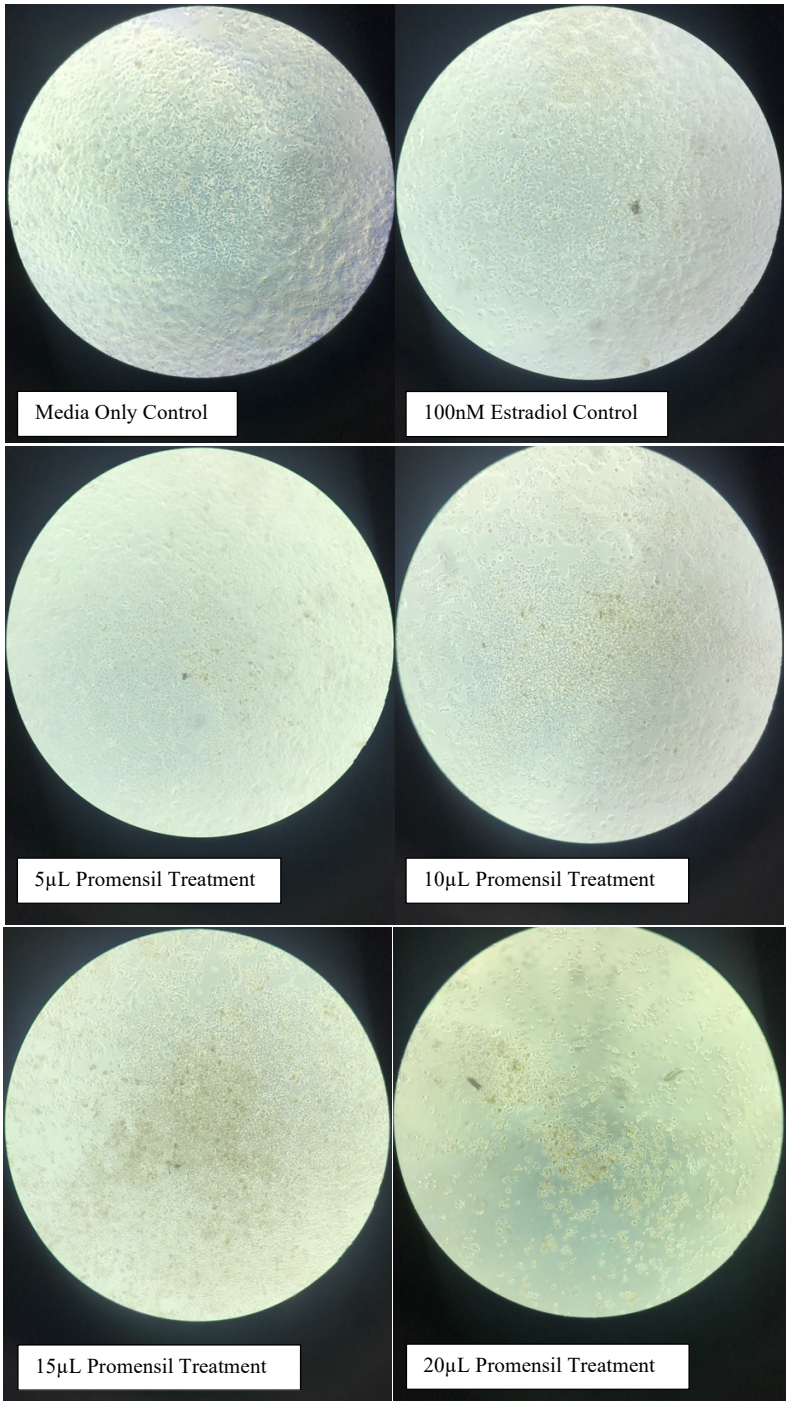

Figure 5: T47D cells after 72 hours of growth in experimental conditions. For all of the cells treated with the Promensil extract, small green particles could be seen in the media when observed under the microscope. These were suspected to be unknown ingredients in the Promensil extract present in the media. Slight differences in density between the treatment groups can also be observed, although the differences observed were not significant.

Cell Counts

T47D Cell Counts

Because the overall objective of this project was to determine the mechanism of action by which Promensil can trigger the previously observed decreased cell proliferation, the first sub-objective for this research was to either confirm or dispute the results of the previous studies, which suggested that Promensil decreases cell proliferation in T47D cells. To do this, viable cell counts were performed on cells from each treatment group after 72 hours of adjustment to the experimental treatments. Since treatments were added to the well plates in triplicate, the average live cell count per treatment group was obtained. The individual results to the three trials of this experiment can be seen in Supplemental Figures S1-3.

Apart from the large deviation in the data for the 10µL Promensil group for Trial 3 (Figure S3), the results from the three trials were fairly consistent. Overall, it can be said with a fair degree of confidence that there exists a relationship between increasing the concentration of the Promensil extract introduced to T47D cells and a decreased cell count after 72 hours of incubation with the Promensil treatments. The use of the 100nM E2 control was also successful, in that in every trial there was an increase in viable cell count in the samples treated with E2 relative to the media only control. To better visualize the relationship between introducing E2 and Promensil to the cells, the average viable cell count per treatment group over all three trials was represented as a percent of the media only control count. This graph can be seen in Figure 6. In establishing this graph, the average cell count from the third trial for the 10 µL Promensil group was omitted, as this data point was taken to be an outlier and not a good representation of the relationship between Promensil concentration and viable cell count, due to the large error within the counts for this treatment group in the third trial. The raw data for all of these counts can be seen in Appendix A.

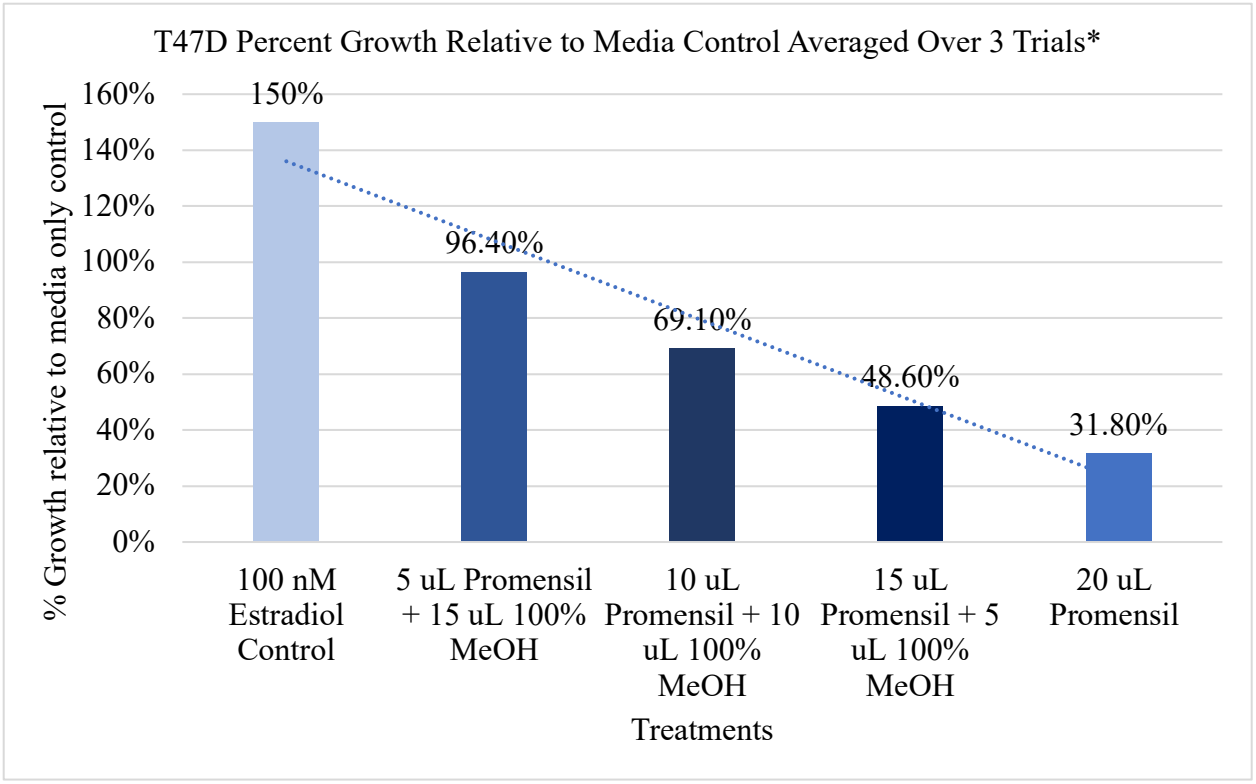

Figure 6: T47D viable cell counts averaged over all three trials and expressed as a percent relative to the media control. Using the average viable cell count per treatment per trial, this number was divided by the average media control viable cell count per trial to obtain the average percent of cell growth per trial relative to the average media control per trial. These numbers were then averaged over all three trials to get the percentages seen in this graph. All the raw data can be seen in Appendix A. **Note that the data from Trial 3 for the 10µL Promensil treatment group was omitted when making this graph, as this data was taken as an outlier to the rest of the trend that was observed during the three trials of this experiment, as seen in the large error bar in Figure S3.*

As seen in Figure 6, the average cell count for the cells introduced to the E2 control was 150% of the media control, suggesting that the presence of E2 stimulated T47D cell proliferation as anticipated. On the other hand, when just 5 µL of Promensil extract was introduced to these cells, the cell counts were about 4% less than the media control (96.4%). Upon each successive addition of 5 µL of Promensil, the cell counts further decreased relative to the media control, in a fairly linear manner. This observed trend of decreased cell counts with increasing Promensil concentration is consistent with the past findings of Wambach and Aquino et. al. (Wambach, 2018, Aquino, et. al., 2019). To investigate what mechanism was driving this decreased proliferation and if the decreased cell count was in response to estrogen receptor interactions, the same cell count procedure was then performed on MDA-MB-231 triple negative breast cancer cells.

MDA-MB-231 Cell Counts

Since MDA-MB-231 cells are a triple negative breast cancer cell line, the cell count experiment was done on this line to establish a negative control. The goal in doing this was to investigate if cells lacking estrogen receptors behaved in a similar manner to the T47D line, which is known to express both ER-α and ER-β. The percent of growth in each treatment group relative to the

media control for this cell line can be seen in Figure 7. The average live cell count per treatment group can be seen in Supplemental Figure S4.

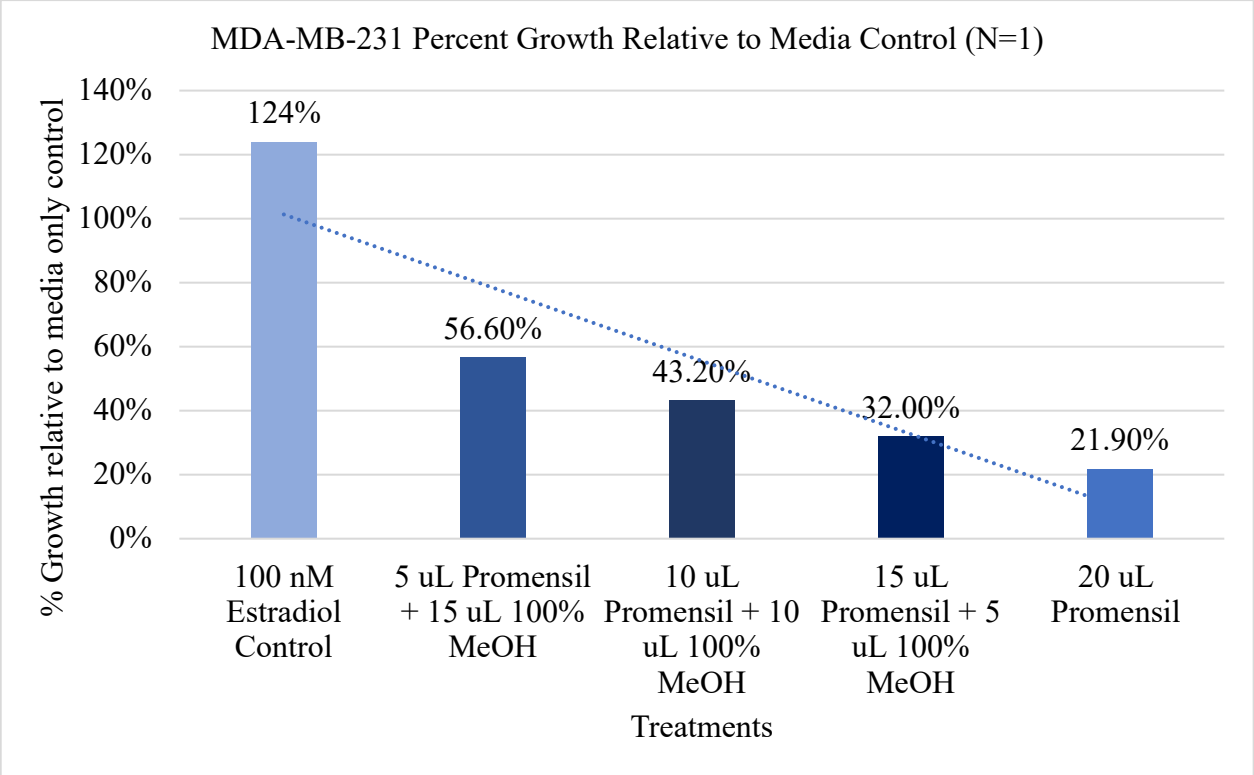

Figure 7: MDA-MB-231 viable cell counts expressed as a percent relative to the media control. Only one trial of this count was performed. The raw data for this count can be seen in Appendix A. Cell count average for each treatment group including the media only control and standard deviation for each group can be seen in Supplemental Figure S4.

Interestingly, the results to this cell count were very similar to the results from the T47D cells. Introducing E2 to the MDA-MB-231 cells resulted in an increased cell count relative to the media control and increasing the concentration of Promensil extract introduced to the cells correlated with decreased cell counts, in a concentration-dependent manner. Since MDA-MB-231 cells are triple negative, it was not expected that E2 would have a stimulatory effect. This is because E2 elicits a proliferative response in ER-positive breast cells via binding to ER-α, which an established triple negative line should not express. So, assuming that MDA-MB-231 cells should lack both ER-α and ER-β but are showing the same response to E2 and Promensil as the T47D cells, this suggests that either the MDA-MB-231 cells are not truly triple negative and may be expressing estrogen receptors, or that the decreased proliferation in both lines is not occurring via an interaction with estrogen receptors at all. Future experiments should look into this first possibility, to assess the validity of MDA-MB-231 cells being truly triple negative. This second possibility however was supported by the previous studies done by Wambach and Aquino et. al., through which it was discovered that when both estrogen receptors were turned off or antagonized, there was no effect on the decreased proliferation that was observed prior, suggesting the decreased proliferation was receptor-independent. (Wambach, 2018, Aquino, et. al. 2019) Moreover, in the Jankowski et. al. 2020 study it was suggested that Promensil is

interacting with estrogen receptors in some manner, but it could not be established if that was what was causing the observed antiproliferation (Jankowski, et. al., 2020).

With the results from these past three studies combined with the present cell count data, it appears that receptor interaction may not be needed for the decreased cell counts. To investigate the possibility that the decreased proliferation observed was receptor-independent, immunoblots were then performed on markers of cell cycle arrest (p21), DNA replication (PCNA), and apoptosis (caspase 3) in T47D cells. Immunoblotting for these three proteins enabled the simultaneous investigation of these three cellular processes, to determine the possibility that the observed cell counts in the T47D cells when exposed to Promensil were either the result of cell cycle arresting, decreased DNA replication and thus decreased cell division, or an early triggering of apoptosis, rather than an ER-α antagonistic or ER-β agonistic mechanism.

Protein Concentration

Prior to preparing the treated T47D cell samples for immunodetection, a protein assay was performed to determine the total protein centration in each sample after 72 hours of incubation with the experimental treatments. The results to this protein assay for the treated T47D cells can be seen in Table 3.

Table 3: Total protein concentration in T47D cells after 72 hours of incubation with experimental treatments.

Treatment	**Total Protein (mg/mL)**
Media Only Control	0.76
100 nM Estradiol Control	0.78
7.5 µL Promensil + 22.5 µL MeOH	0.73
15 µL Promensil + 15 µL MeOH	0.76
22.5 µL Promensil + 7.5 µL MeOH	0.66
30 µL Promensil	0.48

Apart from the protein concentration in the 15 µL Promensil sample, the overall trend of protein concentrations supports the findings from the cell counts. The overall trend for the T47D cell count experiment was an increase in cell count relative to the media control following the introduction of E2 to the cells, and a decreased cell count relative to the media control following the introduction of Promensil to the cells, and the decrease in cell counts also showed a trend of increasingly lower cell counts as the concentration of Promensil increased. Thus, with a higher cell count in the E2 sample, it would be expected for there to be more total protein in this sample when compared to the media control sample, which was observed. Additionally, with the decreasing cell counts in the Promensil groups as Promensil concentration increased, it would be expected that the protein concentrations in these samples would also follow the same decreasing trend, which was also mostly observed. Thus, overall, the results from the protein assay confirmed the results from the cell counts in that the positive control treatment was successful and that there is a relationship between increasing Promensil concentration and a decreased T47D cell count as observed by a lowering total protein concentration, although the reason for this relationship was still unclear. To investigate the mechanism behind this relationship,

immunodetection for PCNA, p21, and caspase 3 was then performed on the treated T47D cells using a slot blot detection method.

Immunodetection

Slot blots were performed on the samples of treated T47D cells for rapid detection of the proteins of interest: PCNA, p21, and caspase 3. These proteins were chosen as targets so that DNA replication, the cell cycle and progression through its check points, and apoptosis were simultaneously examined to determine if Promensil was altering any of these processes to elicit the antiproliferation observed. The results to these slot blots can be seen in Figures 8a-8c.

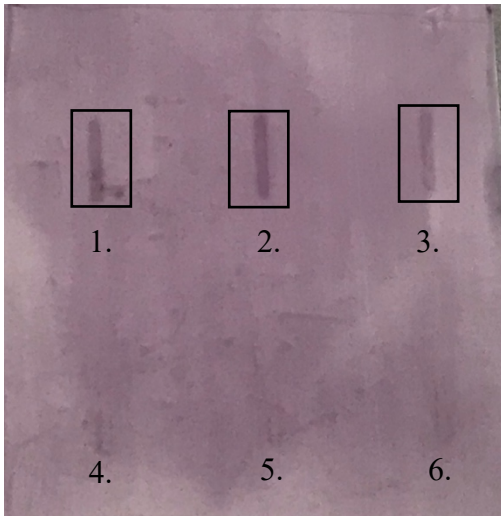

Figure 8a: Immunodetection slot blot on treated T47D cells with anti-PCNA. The numbers on the image correspond to where the treated cell samples were blotted onto the membrane. (Key: 1.) Media only control, 2.) E2 positive control, 3.) 7.5 µL Promensil treatment, 4.) 15 µL Promensil treatment, 5.) 22.5 µL Promensil treatment, 6.) 30 µL Promensil treatment).

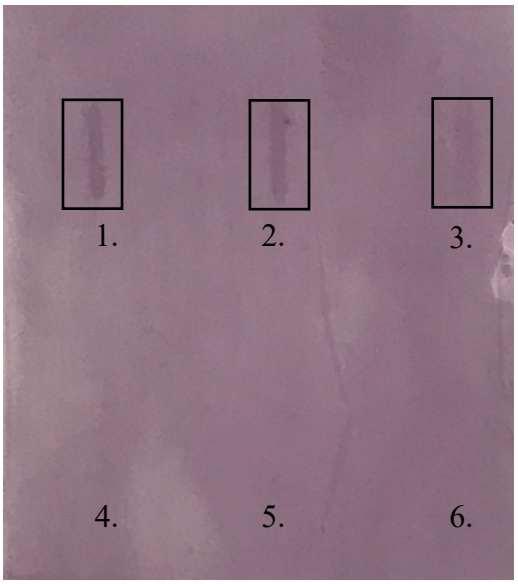

Figure 8b: Immunodetection slot blot on treated T47D cells with anti-p21.

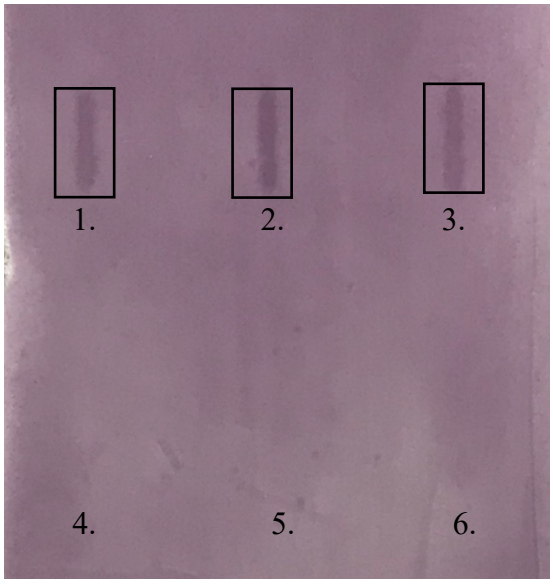

Figure 8c: Immunodetection slot blot on treated T47D cells with anti-caspase 3.

For all three antibodies, only the cells treated with the media only control (1.), E2 control (2.) and the weakest concentration of Promensil (3.) showed detectable levels of protein when 20 µg of total protein from each sample was transferred onto the membrane. The raw densitometry data for each of these bands can be seen in Appendix B. From these blots, it appears that it is possible that DNA replication is downregulated in cells treated with concentrations of Promensil higher than 7.5 µL, since no PCNA detection was observed in samples 4-6 (Figure 8a). Thus, it is possible that downregulated DNA replication is what is triggering the decrease in cell counts. However, the weak expression of p21 in cells treated with 7.5 µL of Promensil and total lack of expression of p21 in cells treated with Promensil at concentrations higher than 7.5 µL (Figure 8b) suggests that arresting the cell cycle at the G1 checkpoint via p21 is not responsible for this downregulation of DNA replication. Thus, I propose that the T47D cells are allowed to progress through the cell cycle through the G1 checkpoint and pass into the S phase, but once in the S

phase, some compound within the Promensil extract triggers a downregulation of PCNA and thus a decreased DNA replication, and this is what is resulting in the decreased cell counts. This is supported by the concept that p21 would normally halt the cell cycle at the G1 checkpoint, so without a detectable expression of p21 in cells treated with Promensil, it is possible that cells are bypassing this checkpoint due to the strong downregulation of p21 present in the cells. These results partially support the initial hypothesis in that DNA replication appears to be decreased in T47D cells treated with concentrations of Promensil higher than 7.5 µL due to the absence of PCNA, yet also negate the part of the hypothesis that proposed that this decrease in DNA replication would be supplemented with an arresting of the cell cycle at the G1 checkpoint due to the presence of p21, which was not detectable in cells treated with Promensil concentrations over 7.5 µL.

The presence of PCNA in the media control and E2 control is largely intuitive: these groups showed the highest levels of cell proliferation, and thus should express the highest levels of PCNA, indicating DNA replication was occurring prior to cell division. Additionally, the cells treated with E2 showed higher levels of proliferation, and also higher levels of PCNA expression compared to the media only control, whereas the cells treated with Promensil had decreased proliferation compared to the media control and also lower levels of PCNA expression as expected (Appendix B). The presence of p21 in the two control samples may suggest that detectable baseline levels of p21 are present in cells dividing under normal growth conditions *in vitro* and when triggered to proliferate via binding to E2. In these instances, p21 would serve to pause the cell cycle at R points to appropriately respond to any DNA damage before proceeding and allowing proliferation to occur in a healthy, checked way. There were no large differences in the levels of p21 expressed by the media control cells and the E2 cells (Appendix B), suggesting that normally dividing cells maintain similar expression levels of p21 to control cell cycle R points when necessary. The weak signal of p21 expression in the cells treated with 7.5 µL of Promensil (Appendix B) and apparent absence of p21 in the cells treated with concentrations of Promensil over 7.5 µL may suggest that some compound in the Promensil extract prevents expression of p21. Moreover, I propose that this downregulation of p21 is causing an imbalance in the cell cycle check point machinery such that cells are allowed to pass through the G1 checkpoint regardless of DNA damage, yet once they enter into the S phase, some component of the Promensil extract is then also preventing normal DNA replication and subsequent cell division via downregulating PCNA expression.

Interestingly, the expression of caspase 3, a marker for cells undergoing apoptosis, was only shown to be expressed in samples 1-3 again (Figure 8c). It was expected that cells with increasingly higher treatments of Promensil would correlate with higher expression levels of caspase 3, suggesting the cells were dying and this was what was causing the decreased cell counts. However, the presence of caspase 3 in the media only control cells may suggest that apoptosis of unhealthy cells is normal under standard growth conditions *in vitro*. The presence of caspase 3 in the E2 control group however is more surprising, since cells in this group had the highest levels of proliferation, so it seems counterintuitive that these cells are also be expressing detectable levels of an apoptosis marker, especially levels that are even higher than the media control (Appendix B). Interestingly, the cells treated with 7.5 µL of Promensil had very similar expression levels of caspase 3 as the E2 control cells (Appendix B), a phenomenon which cannot be explained with the present data. It is possible that there exists a baseline level of apoptosis that

occurs when cells are proliferating at any rate, which could explain the similar expression levels of caspase 3 present in the media control and E2 cells. However, overall, the lack of expression of caspase 3 in cells treated with concentrations of Promensil over 7.5 μL does not support the original hypothesis that suggested the decreased cell counts in cells treated with Promensil is due to an early triggering of apoptosis, suggesting that the observed decrease in cell counts is likely due to a decrease in proliferation rather than an increase in apoptosis.

Overall, the data from both the cell count and immunodetection experiments suggests that introducing Promensil to T47D breast epithelial cells correlates with decreased cell counts in a concentration-dependent manner (Figure 6). The observation of Promensil's antiproliferative effects were supported by protein assays, which displayed that the overall trend in total protein concentration was a progressive decrease associated with increasing levels of Promensil treatments (Table 3). The mechanism behind this antiproliferation is suggested to be apoptosis-independent, but rather related to decreased DNA replication in the S phase of the cell cycle, suggested by the lack of expression of PCNA, p21, and caspase 3 in T47D cells treated with Promensil extracts at a concentration higher than 7.5 μL (Figures 8a-c). However, it is important to note that the immunodetection method described in this report did not separate proteins based on size prior to antibody treatment. As such, nonspecific binding between proteins other than the target proteins and the antibodies used for detection is a possibility. However, adequate care was taken in blocking nonspecific binding between non-target proteins and the antibodies, so it can be said with a fair degree of confidence that the expression patterns in Figures 8a-c do represent the target proteins. Additionally, it must also be taken into consideration that present in the Promensil extract are ingredients other than phytoestrogens that are also soluble in methanol. Thus, while I can claim that the data suggests Promensil is interacting with T47D cells via the aforementioned mechanism, no claim can be made that it is the phytoestrogens within the Promensil themselves triggering the antiproliferation. Additionally, the immunodetection that was done for PCNA, p21, and caspase 3 with the T47D cells was only performed once, and with an N=1 no strong claim can actually be made about the level of expression of these proteins in response to Promensil and what this means in terms of its interaction with DNA replication, the cell cycle, or apoptosis.

Recommendations

Future studies should repeat the immunodetection for PCNA, p21, and caspase 3 on the T47D cells since only one trial of this protocol was performed. Moreover, separation techniques should be employed during the Promensil extraction process to separate the four phytoestrogen components of Promensil from any other methanol-soluble components. In doing so, it could better be investigated if the phytoestrogens themselves or some other compound are eliciting the antiproliferation seen with T47D and MDA-MB-231 cells treated with Promensil extract. Separation could even be further employed to separate the four phytoestrogen components themselves to see if there is a different response in cells treated with either daidzein, genistein, biochanin A, or formononetin.

Additionally, MDA-MB-231 cells were used as a negative control line in this study since they are reportedly triple negative. However, they responded to the treatments with the same relationship as T47D cells, and even showed increased proliferation when treated with E2 (Figure 7), which should not occur in a cell line without estrogen receptors. As such, determining the receptor status for these cells via immunodetection for ER-α and ER-β should be a priority for future studies. Additionally, immunodetection for p21, PCNA, and caspase 3 should be performed on MDA-MB-231 cells, as was done on the T47D cells. If the MDA-MB-231 cells do not show expression of ER-α and ER-β and show similar patterns of expression for PCNA, p21, and caspase 3 as T47D, this would reinforce the mechanism proposed here for antiproliferation in breast epithelial cells in response to Promensil being an estrogen receptor-independent mechanism of decreased DNA replication in the S phase of the cell cycle after the G1 checkpoint has been traversed.

References

About Promensil. (n.d.). Retrieved from https://Promensil.co.uk/about/

Aquino, M., Ellis, A., & Giansiracusa, S. (2019) Relationship between Promensil and estrogen receptor alpha in breast cancer cells. Worcester Polytechnic Institute.

ATCC. (n.d.). MCF 10F (ATCC® CRL-10318™). Retrieved from https://www.atcc.org/Products/All/CRL-10318.aspx#characteristics

ATCC. (n.d.). MDA-MB-231 (ATCC® HTB-26™). Retrieved from https://www.atcc.org/products/all/htb-26.aspx

ATCC. (n.d.). T-47D (ATCC® HTB-133™). Retrieved from https://www.atcc.org/products/all/HTB-133.aspx

Atkinson, C., Warren, R. M., Sala, E., Dowsett, M., Dunning, A. M., Healey, C. S., Runswick, S., Day, N. E., & Bingham, S. A. (2004). Red-clover-derived isoflavones and mammographic breast density: a double-blind, randomized, placebo-controlled trial [ISRCTN42940165]. *Breast cancer research: BCR*, *6*(3), R170–R179. https://doi.org/10.1186/bcr773

Banks, E., Beral, V., Bull, D., Reeves, G., Austoker, J., English, R., Patnick, J., Peto, R., Vessey, M., Wallis, M., Abbott, S., Bailey, E., Baker, K., Balkwill, A., Barnes, I., Black, J., Brown, A., Cameron, B., Canfell, K., … Timadjer, A. (2003). Breast cancer and hormone-replacement therapy in the Million Women Study. *The Lancet (British Edition), 362*(9382), 419–427. https://doi.org/10.1016/s0140-6736(03)14065-2

Boehm, E. M., Gildenberg, M. S., & Washington, M. T. (2016). The Many Roles of PCNA in Eukaryotic DNA Replication. *The Enzymes*, *39*, 231–254. https://doi.org/10.1016/bs.enz.2016.03.003

Biorad. (n.d.). Image Lab Software User Guide. Version 6.1.

Cagnacci, A., & Venier, M. (2019). The Controversial History of Hormone Replacement Therapy. *Medicina (Kaunas, Lithuania)*, *55*(9), 602. https://doi.org/10.3390/medicina55090602

Centers for Disease Control and Prevention. (n.d.). USCS Data Visualizations - CDC. Retrieved from https://gis.cdc.gov/Cancer/USCS/DataViz.html

Couse, J.F., & Korach, K.S. (1999). Estrogen Receptor Null Mice: What Have We Learned and Where Will They Lead Us? *Endocrine Reviews, 20*(3), 358-417 https://doi.org/10.1210/edrv.20.3.0370

Ding, L., Cao, J., Lin, W., Chen, H., Xiong, X., Ao, H., … Cui, Q. (2020). The Roles of Cyclin-Dependent Kinases in Cell-Cycle Progression and Therapeutic Strategies in Human Breast Cancer. *International Journal of Molecular Sciences*, *21*(6), 1960. doi:10.3390/ijms21061960

Estradiol. (2005). Retrieved from https://go.drugbank.com/drugs/DB00783

Estrogen. (2018). Retrieved from https://www.hormone.org/your-health-and-hormones/glands-and-hormones-a-to-z/hormones/estrogen

European Collection of Authenticated Cell Cultures. (2017). Cell line profile: MDA-MB-231. Retrieved from https://www.phe-culturecollections.org.uk/media/133182/mda-mb-231-cell-line-profile.pdf

Giacinti, C., Giordano, A. (2006). RB and cell cycle progression. *Oncogene, 25*, 5220–5227. https://doi.org/10.1038/sj.onc.1209615

Hamilton, K. J., Hewitt, S. C., Arao, Y., & Korach, K. S. (2017). Estrogen Hormone Biology. *Current topics in developmental biology*, *125*, 109–146. https://doi.org/10.1016/bs.ctdb.2016.12.005

Harvard Health Publishing. (2019). Perimenopause: Rocky road to menopause. Retrieved from https://www.health.harvard.edu/womens-health/perimenopause-rocky-road-to-menopause

Ingram, D., Sanders, K., Kolybaba, M., & Lopez, D. (1997). Case-control study of phyto-oestrogens and breast cancer. *Lancet (London, England)*, *350*(9083), 990–994. https://doi.org/10.1016/S0140-6736(97)01339-1

Jankowksi, M., Sullivan, S., & Zarate, C. (2020) Effect of Promensil on T47D breast cancer cells with respect to estrogen receptors alpha and beta. Worcester Polytechnic Institute.

Khan, S. A., Chatterton, R. T., Michel, N., Bryk, M., Lee, O., Ivancic, D., Heinz, R., Zalles, C. M., Helenowski, I. B., Jovanovic, B. D., Franke, A. A., Bosland, M. C., Wang, J., Hansen, N. M., Bethke, K. P., Dew, A., Coomes, M., & Bergan, R. C. (2012). Soy isoflavone supplementation for breast cancer risk reduction: a randomized phase II trial. *Cancer prevention research (Philadelphia, Pa.)*, *5*(2), 309–319. https://doi.org/10.1158/1940-6207.CAPR-11-0251

Klinge C. M. (2001). Estrogen receptor interaction with estrogen response elements. *Nucleic acids research*, *29*(14), 2905–2919. https://doi.org/10.1093/nar/29.14.2905

Křížová, L., Dadáková, K., Kašparovská, J., & Kašparovský, T. (2019). Isoflavones. Molecules (Basel, Switzerland), 24(6), 1076–. https://doi.org/10.3390/molecules24061076

Lee, H. R., Kim, T. H., & Choi, K. C. (2012). Functions and physiological roles of two types of estrogen receptors, ERα and ERβ, identified by estrogen receptor knockout mouse. *Laboratory animal research*, *28*(2), 71–76. https://doi.org/10.5625/lar.2012.28.2.71

Menopause. (2020, October 14). Retrieved from https://www.mayoclinic.org/diseases-conditions/menopause/symptoms-causes/syc-20353397?utm_source=Google&utm_medium=abstract&utm_content=Menopause&utm_campaign=Knowledge-panel

National Cancer Institute. (2017). Hormone Therapy for Breast Cancer Fact Sheet. Retrieved from https://www.cancer.gov/types/breast/breast-hormone-therapy-fact-sheet

National Institute of Health. (n.d.) What Is Menopause? Retrieved from https://www.nia.nih.gov/health/what-menopause

Paterni, I., Granchi, C., Katzenellenbogen, J. A., & Minutolo, F. (2014). Estrogen receptors alpha (ERα) and beta (ERβ): subtype-selective ligands and clinical potential. *Steroids*, *90*, 13–29. https://doi.org/10.1016/j.steroids.2014.06.012

Russo, I., & Russo, J. (1996). Mammary Gland Neoplasia in Long-Term Rodent Studies. *Environmental Health Perspectives, 104*(9), 938-967. doi:10.2307/3433143

Russo, J., Fernandez, S.V., Russo, P.A., Fernbaugh, R., Sheriff, F.S., Lareef, H.M., Garber, J. and Russo, I.H. (2006). 17-Beta-Estradiol induces transformation and tumorigenesis in human breast epithelial cells. *The FASEB Journal*, *20*(10), 1622-1634. doi:10.1096/fj.05-5399

Sakamoto, T., Horiguchi, H., Oguma, E., & Kayama, F. (2010). Effects of diverse dietary phytoestrogens on cell growth, cell cycle and apoptosis in estrogen-receptor-positive breast cancer cells. *The Journal of nutritional biochemistry*, *21*(9), 856–864. https://doi.org/10.1016/j.jnutbio.2009.06.010

Santa Cruz Biotechology (n.d.). caspase-3 p17 Antibody (B-4): sc-271028. Retrieved from https://www.scbt.com/p/caspase-3-p17-antibody-b-4?requestFrom=search

Santa Cruz Biotechnology. (n.d.) PCNA Antibody (F-2): sc-25280. Retrieved from https://www.scbt.com/p/pcna-antibody-f-2?requestFrom=search

Santa Cruz Biotechnology. (n.d.). p21 Waf1/Cip1 Antibody (F-5): sc-6246. Retrieved from https://www.scbt.com/p/p21-antibody-f-5?requestFrom=search

Sar, M., & Welsch, F. (1999). Differential expression of estrogen receptor-beta and estrogen receptor-alpha in the rat ovary. *Endocrinology*, *140*(2), 963–971. https://doi.org/10.1210/endo.140.2.6533

Schultz-Norton, J. R., Gabisi, V. A., Ziegler, Y. S., McLeod, I. X., Yates, J. R., & Nardulli, A. M. (2007). Interaction of estrogen receptor alpha with proliferating cell nuclear antigen. *Nucleic acids research*, *35*(15), 5028–5038. https://doi.org/10.1093/nar/gkm533

Sigma Aldrich. (n.d.). Insulin solution from bovine pancreas. Retrieved from https://www.sigmaaldrich.com/catalog/product/sigma/i0516?lang=en&region=US

Sigma Aldrich (n.d.). SIGMA*FAST* BCIP/NBT. Retrieved from https://www.sigmaaldrich.com/catalog/product/sigma/B5655?lang=en&region=US&gclid=Cj0KCQiA4feBBhC9ARIsABp_nbV33D8r5hlY7pt8oRBIAOEkG-7aFGbfDHxgDct_IsTbImtmGNJw8-gaAhS-EALw_wcB

Wambach, R. (2018). Effect of Promensil on breast cancer cells in regard to the estrogen receptor beta. Worcester Polytechnic Institute.

Weinberg, A. (2014). *The Biology of Cancer* (2nd ed.). New York: Garland Science.

Welshons, W. V., Wolf, M. F., Murphy, C. S., & Jordan, V. C. (1988). Estrogenic activity of phenol red. *Molecular and cellular endocrinology*, *57*(3), 169–178. https://doi.org/10.1016/0303-7207(88)90072-x

Xiong, X. Y., Hu, X. J., Li, Y., & Liu, C. M. (2015). Inhibitory Effects of Enterolactone on Growth and Metastasis in Human Breast Cancer. *Nutrition and cancer*, *67*(8), 1324–1332. https://doi.org/10.1080/01635581.2015.1082113

Xu, X., Duncan, A. M., Merz, B. E., & Kurzer, M. S. (1998). Effects of soy isoflavones on estrogen and phytoestrogen metabolism in premenopausal women. *Cancer Epidemiology and Prevention Biomarkers*, 7(12), 1101-1108.

Supplemental Figures

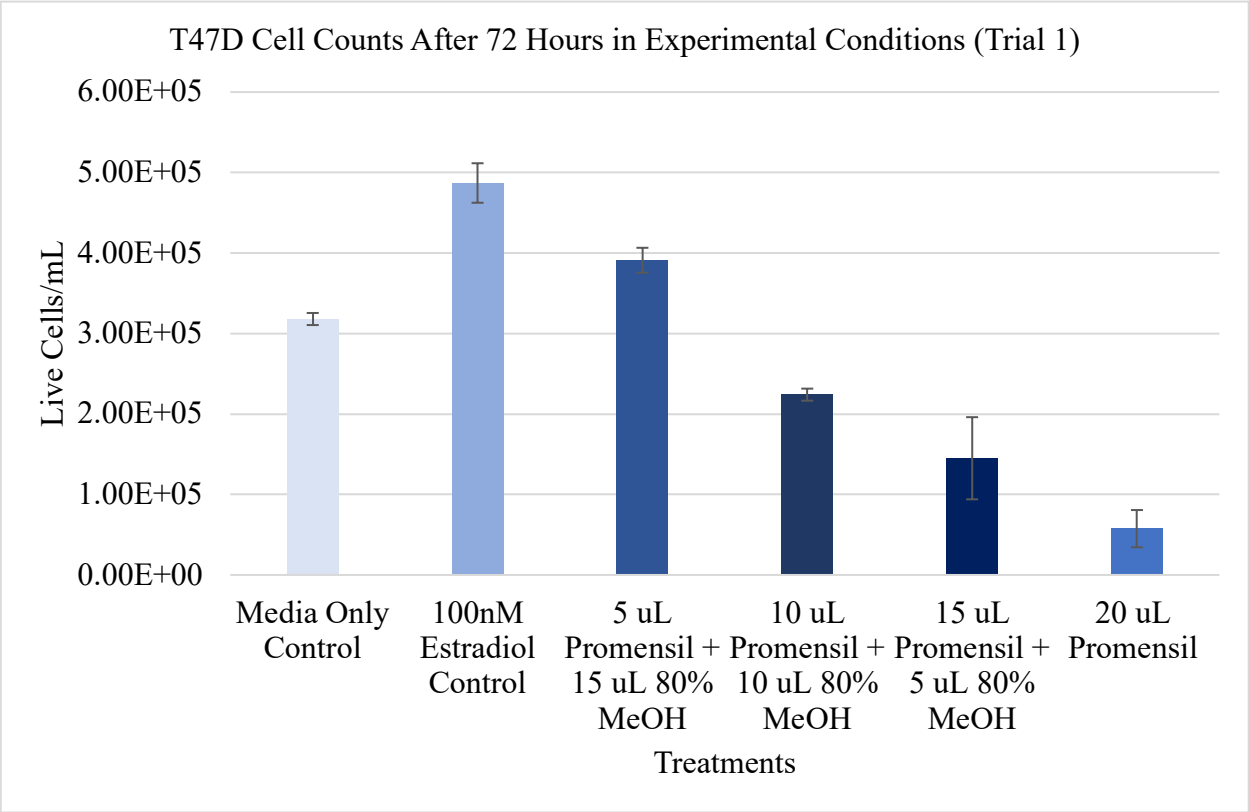

Figure S1: Viable cell concentration (live cells/mL) for Trial 1 of cell count experiment with T47D cells. All cells were synchronized to the same stage in the cell cycle by allowing them to adjust to serum-free media for 24 hours (DMEM + 1% P/S, 0.08% insulin). Cells were then left to adjust to the experimental media for another 24 hours (phenol red-free DMEM + 10% charcoal stripped FBS, 1% P/S, 0.08% insulin). The experimental treatments were then added to the cells in triplicate. The average live cell count for each treatment group is represented in this graph. The error bars represent the standard deviation. 80% MeOH was added to the 5, 10, and 15 uL Promensil treatments to control for the amount of MeOH introduced by the Promensil treatments themselves, since the Promensil extract was contained in 80% MeOH. All raw data for this trial can be seen in Appendix A.

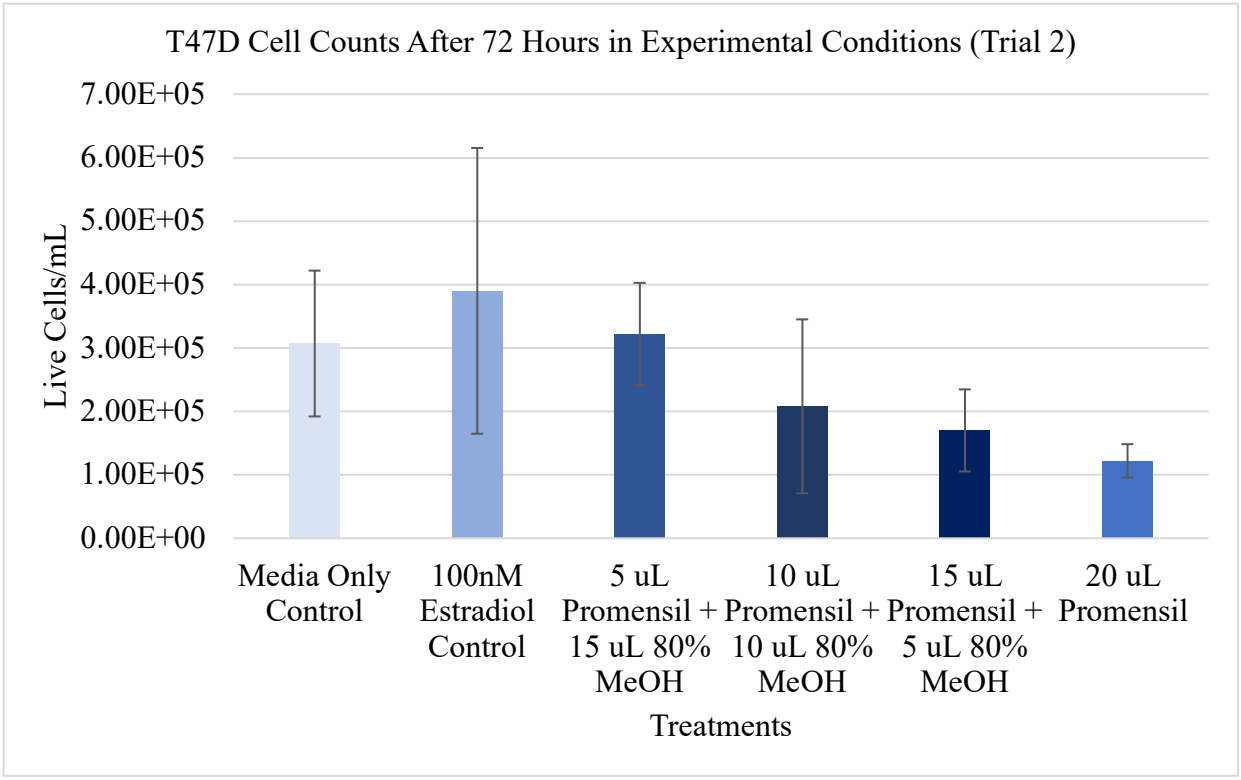

Figure S2: Second trial of cell count experiment with T47D cells. All raw data for this trial can be seen in Appendix A.

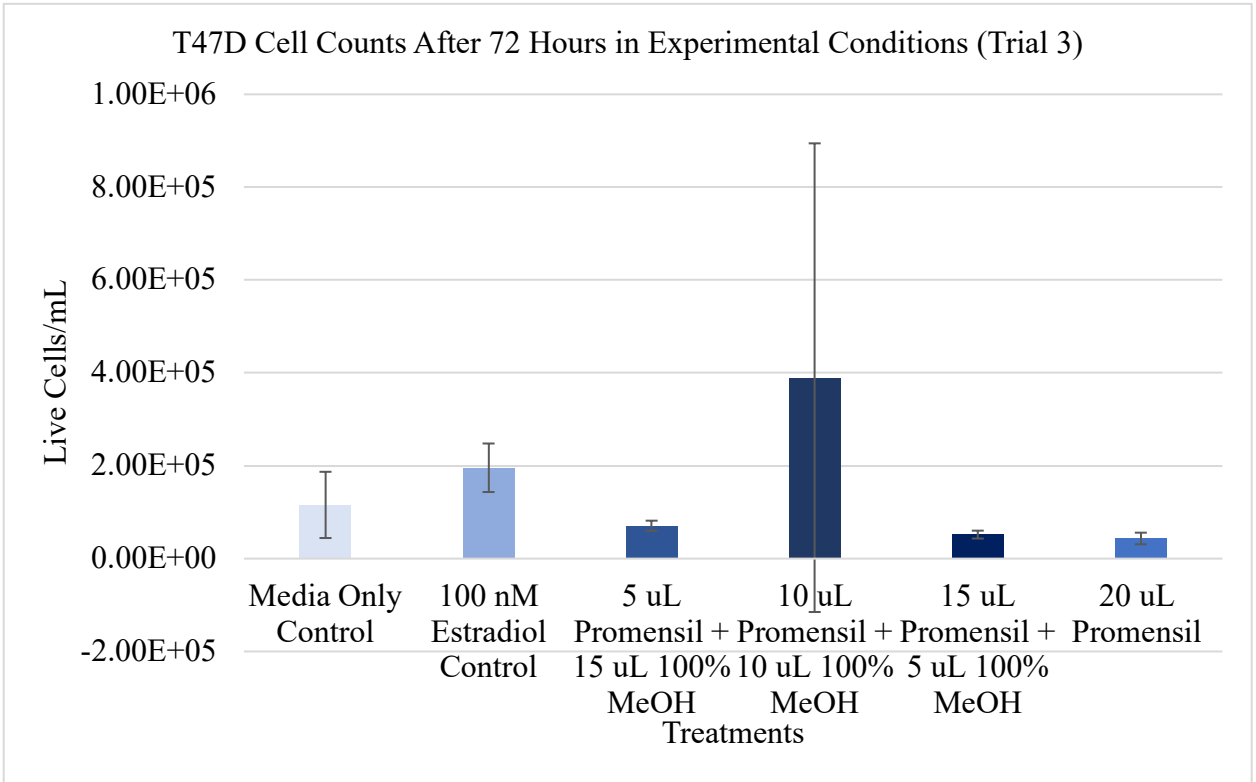

Figure S3: Third trial of cell count experiment with T47D cells. All raw data for this trial can be seen in Appendix A.

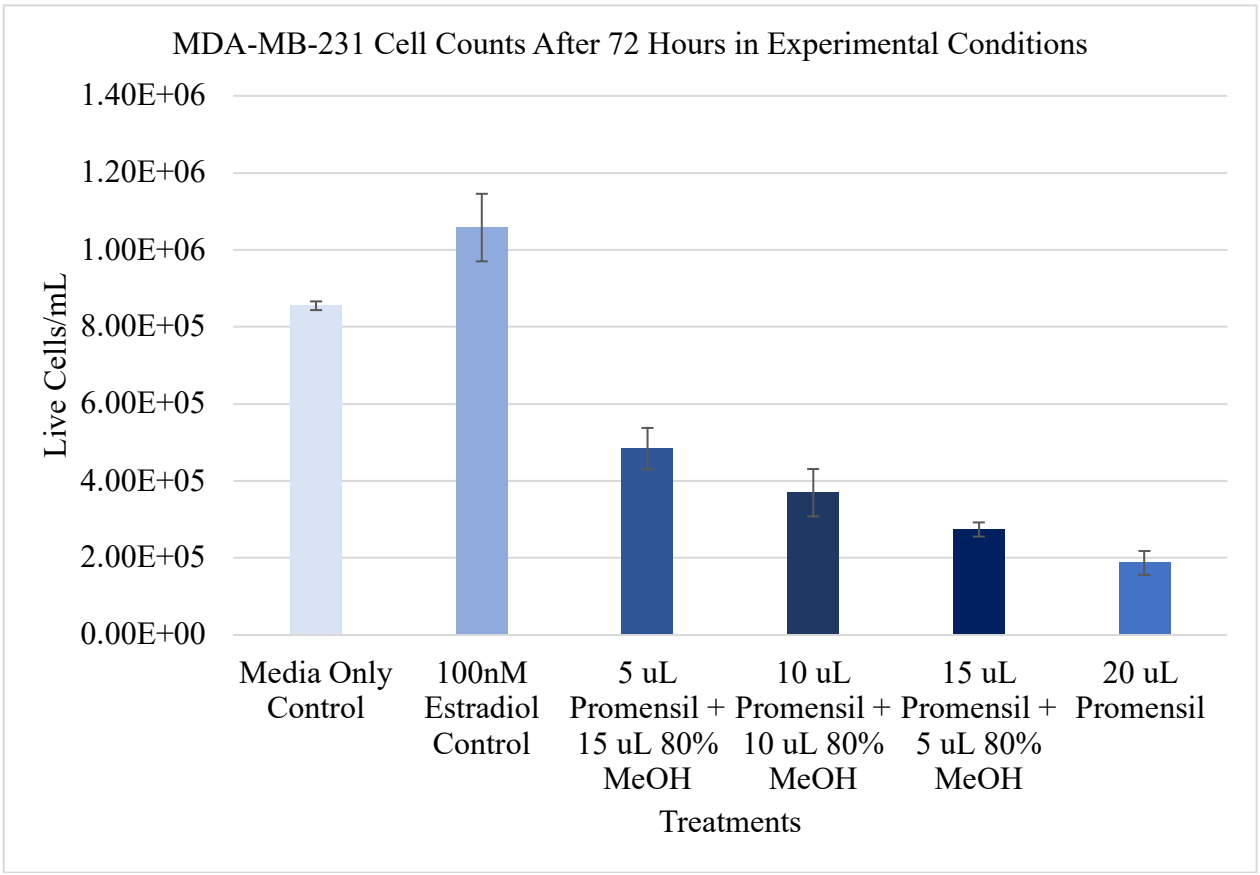

Figure S4: MDA-MB-231 viable cell concentration (live cells/mL) for the cell count experiment with the negative control line. All cells were synchronized to the same stage in the cell cycle by allowing them to adjust to serum-free media for 72 hours (DMEM + 1% P/S). Cells were then left to adjust to the experimental media for another 24 hours (phenol red-free DMEM + 10% charcoal stripped FBS, 1% P/S). The experimental treatments were then added to cells in duplicate. The average live cell count for each experimental treatment is represented in this graph. The error bars represent the standard deviation. 80% MeOH was added to the 5, 10, and 15 µL Promensil treatments to control for the amount of MeOH introduced by the Promensil treatments themselves, since the Promensil extract was contained in 80% MeOH. All raw data for this trial can be seen in Appendix A.

Appendix A: Cell Count Raw Data

T47D Cell Counts Trial 1

Media Only Control	**100 nM Estradiol Control**	**5 uL Promensil + 15 uL 100% MeOH**	**10 uL Promensil + 10 uL 100% MeOH**	**15 uL Promensil + 5 uL 100% MeOH**	**20 uL Promensil**	
3.18E+05	4.59E+05	4.09E+05	2.31E+05	2.02E+05	4.70E+04	
3.26E+05	5.01E+05	3.85E+05	2.16E+05	1.31E+05	8.40E+04	
3.11E+05	5.02E+05	3.80E+05	2.24E+05	1.03E+05	4.14E+04	
3.18E+05	4.87E+05	3.91E+05	2.24E+05	1.45E+05	5.75E+04	**Average**
7505.553499	24542.48018	15502.68794	7505.553499	51032.66928	23148.50607	**Standard Deviation**

T47D Cell Counts Trial Two

Media Only Control	**100 nM Estradiol Control**	**5 uL Promensil + 15 uL 100% MeOH**	**10 uL Promensil + 10 uL 100% MeOH**	**15 uL Promensil + 5 uL 100% MeOH**	**20 uL Promensil**	
2.44E+05	3.43E+05	2.57E+05	1.67E+05	2.25E+05	1.51E+05	
4.40E+05	6.35E+05	2.96E+05	9.62E+04	9.89E+04	1.00E+05	
2.38E+05	1.92E+05	4.12E+05	3.61E+05	1.87E+05	1.14E+05	
3.07E+05	3.90E+05	3.22E+05	2.08E+05	1.70E+05	1.22E+05	**Average**
114931.8639	225208.792	80624.6447	137093.4474	64687.47947	26350.20557	**Standard Deviation**

T47D Cell Counts Trial Three

Media Only Control	**100 nM Estradiol Control**	**5 uL Promensil + 15 uL 100% MeOH**	**10 uL Promensil + 10 uL 100% MeOH***	**15 uL Promensil + 5 uL 100% MeOH**	**20 uL Promensil**	
1.28E+05	2.56E+05	6.44E+04	1.19E+05	6.11E+04	5.53E+04	
3.90E+04	1.64E+05	6.46E+04	7.81E+04	4.96E+04	4.45E+04	
1.80E+05	1.67E+05	8.34E+04	9.72E+05	4.45E+04	3.04E+04	
1.16E+05	1.96E+05	7.08E+04	3.90E+05	5.17E+04	4.34E+04	**Average**
71304.51131	52271.72595	10912.37829	504701.0699	8503.136676	12486.39259	**Standard Deviation**

*The data for this column (10 uL Promensil treatment) was excluded when graphing the percentage of cell growth relative to the media control for the next data analysis portion because it was deemed an outlier due to the extremely large standard deviation.

T47D Cell Counts Averaged Over All Trails and Expressed as Percent Relative to Media Control

	Trial 1 Average % of Media Control	**Trial 2 Average % of Media Control**	**Trial 3 Average % of Media Control**	**Average over 3 Trials**	**Standard Deviation**
100 nM Estradiol Control	153%	127%	169%	150%	21.26461691
5 uL Promensil + 15 uL 100% MeOH	123%	105%	61.2%	96.40%	31.74534888
10 uL Promensil + 10 uL 100% MeOH	70.4%	67.8%	***omitted**	69.10%	1.90056767
15 uL Promensil + 5 uL 100% MeOH	45.6%	55.4%	44.7%	48.60%	5.912397807
20 uL Promensil	18.1%	39.7%	37.5%	31.80%	11.91553911

MDA-MB-231 Cell Counts Trial 1

Media Only Control	**100 nM Estradiol Control**	**5 uL Promensil + 15 uL 100% MeOH**	**10 uL Promensil + 10 uL 100% MeOH**	**15 uL Promensil + 5 uL 100% MeOH**	**20 uL Promensil**	
8.47E+05	1.12E+06	5.22E+05	4.13E+05	2.87E+05	2.09E+05	
8.63E+05	9.96E+05	4.46E+05	3.26E+05	2.61E+05	1.65E+05	
8.55E+05	1.06E+06	4.84E+05	3.70E+05	2.74E+05	1.87E+05	**Average**
11313.7085	87681.24087	53740.11537	61518.28996	18384.77631	31112.69837	**Standard Deviation**

Appendix B: Immunoblot Densitometry Raw Data

PCNA Blot Densitometry Raw Data

No.	Label	Type	Volume (Int)	Adj. Vol. (Int)	Mean Bkgd. (Int)	Abs. Quant.
1	Media Only Control	Unknown	4,768,267.00	-305,849.33	131.8192	N/A
2	E2 Control	Unknown	4,827,957.00	-369,354.77	129.82569	N/A
3	7.5 uL Promensil	Unknown	5,121,956.00	-170,796.56	140.16824	N/A

Rel. Quant.	# of Pixels	Min. Value (Int)	Max. Value (Int)	Mean Value (Int)	Std. Dev.	Area (mm2)
N/A	38493	75	148	123.873613	12.629885	275.934952
N/A	40033	91	144	120.59943	10.73608	286.974357
N/A	37760	104	164	135.645021	12.336644	270.680482

p21 Blot Densitometry Raw Data

No.	Label	Type	Volume (Int)	Adj. Vol. (Int)	Mean Bkgd. (Int)	Abs. Quant.
1	Media Only Control	Unknown	4,045,492.00	-127,990.75	128.33588	N/A
2	E2 Control	Unknown	4,173,439.00	-152,464.81	128.38415	N/A
3	7.5 uL Promensil	Unknown	3,338,465.00	-91,919.18	126.8258	N/A

Rel. Quant.	# of Pixels	Min. Value (Int)	Max. Value (Int)	Mean Value (Int)	Std. Dev.	Area (mm2)
N/A	32520	104	139	124.400123	6.151525	233.11783
N/A	33695	90	138	123.859297	6.569215	241.540753
N/A	27048	100	138	123.427425	4.082155	193.892099

Caspase 3 Blot Densitometry Raw Data

No.	Label	Type	Volume (Int)	Adj. Vol. (Int)	Mean Bkgd. (Int)	Abs. Quant.
1	Media Only Control	Unknown	5,172,106.00	-186,191.07	129.20277	N/A
2	E2 Control	Unknown	3,821,976.00	-236,795.85	124.53659	N/A
3	7.5 uL Promensil	Unknown	3,979,205.00	-229,083.75	130.53005	N/A

Rel. Quant.	# of Pixels	Min. Value (Int)	Max. Value (Int)	Mean Value (Int)	Std. Dev.	Area (mm2)
N/A	41472	105	137	124.713204	7.344076	297.289749
N/A	32591	93	136	117.270903	8.959578	233.62679
N/A	32240	102	147	123.424473	8.061369	231.110665